Provided for non-commercial research and education use.
Not for reproduction, distribution or commercial use.

ELSEVIER

Volume 82 1 July 2014 ISSN 0278-4343

CONTINENTAL SHELF RESEARCH

Editors:
Michael Collins
Southampton, UK

Richard W. Sternberg
Seattle, WA, USA

www.elsevier.com/locate/csr

This article appeared in a journal published by Elsevier. The attached copy is furnished to the author for internal non-commercial research and education use, including for instruction at the authors institution and sharing with colleagues.

Other uses, including reproduction and distribution, or selling or licensing copies, or posting to personal, institutional or third party websites are prohibited.

In most cases authors are permitted to post their version of the article (e.g. in Word or Tex form) to their personal website or institutional repository. Authors requiring further information regarding Elsevier's archiving and manuscript policies are encouraged to visit:

http://www.elsevier.com/authorsrights

Author's personal copy

Continental Shelf Research 82 (2014) 37–42

Contents lists available at ScienceDirect

Continental Shelf Research

journal homepage: www.elsevier.com/locate/csr

Research papers

Observations of wave effects on inlet circulation

Mara Orescanin [a,b,*], Britt Raubenheimer [a], Steve Elgar [a]

[a] Woods Hole Oceanographic Institution, 266 Woods Hole Rd., Woods Hole, MA 02543, USA
[b] Department of Mechanical Engineering, Massachusetts Institute of Technology, 77 Massachusetts Ave, Cambridge, MA 02139, USA

ARTICLE INFO

Article history:
Received 7 September 2013
Received in revised form
24 March 2014
Accepted 4 April 2014
Available online 24 April 2014

Keywords:
Tidal inlet hydrodynamics
Wave effects on inlets
Multiple inlets

ABSTRACT

Observations of water levels, winds, waves, and currents in Katama Bay, Edgartown Channel, and Katama Inlet on Martha's Vineyard, Massachusetts are used to test the hypothesis that wave forcing is important to circulation in inlet channels of two-inlet systems and to water levels in the bay between the inlets. Katama Bay is connected to the Atlantic Ocean via Katama Inlet and to Vineyard Sound via Edgartown Channel. A numerical model based on the momentum and continuity equations that uses measured bathymetry and is driven with observed water levels in the ocean and sound, ocean waves, and local winds predicts the currents observed in Katama Inlet more accurately when wave forcing is included than when waves are ignored. During Hurricanes Irene and Sandy, when incident (12-m water depth) significant wave heights were greater than 5 m, breaking-wave cross-shore (along-inlet-channel) radiation stress gradients enhanced flows from the ocean into the bay during flood tides, and reduced (almost to zero during Irene) flows out of the bay during ebb tides. Model simulations without the effects of waves predict net discharge from the sound to the ocean both during Hurricane Irene and over a 1-month period with a range of conditions. In contrast, simulations that include wave forcing predict net discharge from the ocean to the sound, consistent with the observations.

© 2014 Elsevier Ltd. All rights reserved.

1. Introduction

Inlets are common coastal features connecting bays and estuaries with the open ocean. Flows through inlets can transport sediments, pollutants, nutrients, and other materials both into and out of the bay, affecting navigation, recreation, and water quality. Although flows in inlets often are driven by tides, the effects of ocean surface gravity waves on the circulation, morphology, and stability of inlet channels have been hypothesized for decades (Stevenson, 1886; LeConte, 1905; O'Brien, 1931, 1969; Bruun, 1978). Recently the importance of ocean surface waves to inlet dynamics has been investigated with numerical models (Bertin et al., 2009; Malhadas et al., 2009; Olabarrieta et al., 2011; Dodet et al., 2013).

As wind-generated surface waves (swell and sea) break in the shallow water depths on the ebb shoals offshore of inlet mouths and on the beaches alongshore of the inlet, their momentum is transferred to the water column. Gradients in wave radiation stresses caused by wave breaking can raise water levels (setup) near the shoreline (Longuet-Higgins and Stewart, 1964), and drive alongshore currents if incident waves propagate at an angle to the shoreline (Longuet-Higgins, 1970). Unlike an ocean beach, there is no physical barrier at an inlet mouth, and thus wave radiation stress gradients have been hypothesized to drive flow into the inlet channel, raising water levels in the bay (Bertin et al., 2009; Malhadas et al., 2009; Olabarrieta et al., 2011; Dodet et al., 2013). Similarly, wave-induced setup along the shoreline to the sides of inlet channels can produce areas of relatively high water level compared with the level in the channel, also driving water toward the inlet mouth (Apotsos et al., 2008; Malhadas et al., 2009).

Although theory and numerical models (Bertin et al., 2009; Malhadas et al., 2009; Olabarrieta et al., 2011; Dodet et al., 2013) suggest waves can affect water levels and currents near and within inlets, there are few observational tests of these hypotheses. Recent numerical results (Bertin et al., 2009; Malhadas et al., 2009; Olabarrieta et al., 2011; Dodet et al., 2013) show an increase in bay water levels and changes to inlet flows resulting from surface gravity waves.

There have been many studies of bays with two or more inlets, but most have considered systems with the same tidal forcing at all the inlets and have focused on morphological stability (Bruun and Adams, 1988; Aubrey and Giese, 1993; Salles et al., 2005; van de Kreeke et al., 2008). Straits forced by different tides on either end also have been investigated (Campbell et al., 1998; Stevens et al., 2008; Easton et al., 2012), but wave effects were not included.

Here, observations of water levels, winds, waves, and currents in Katama Inlet and Bay, MA (Fig. 1), including those during Hurricanes Irene and Sandy, combined with a numerical implementation of the momentum and continuity equations (Malhadas et al., 2009)

* Corresponding author. Tel.: +1 206 940 5694.
E-mail address: mara.orescanin@gmail.com (M. Orescanin).

http://dx.doi.org/10.1016/j.csr.2014.04.010
0278-4343/© 2014 Elsevier Ltd. All rights reserved.

Author's personal copy

extended to account for different tidal forcing at either end of Katama Bay are shown to be consistent with the hypothesis that wave radiation stresses result in increased flow into the inlet.

2. Theory and model

Simplifying the governing equations to a first-order approximation, the hydrodynamics of the Katama Bay system, including Edgartown Channel and Katama Inlet, are described by the cross-shore momentum balance and continuity (mass conservation). Nonlinear-advective terms, to a first order approximation, are assumed to cancel (Jay, 1991; Olabarrieta et al., 2011) or to be small (Lentz et al., 1999). Given the small spatial scales, Coriolis terms are small. Therefore, the depth-averaged, cross-shore (along-inlet) momentum balance for each inlet is (Proudman, 1953; Campbell et al., 1998; Malhadas et al., 2009)

$$\frac{\partial Q}{\partial t} = \nabla P - C_d \frac{|Q|Q}{A^2} b + R_s b + \frac{\rho_a}{\rho_w} \tau_w b \tag{1}$$

where Q is the volume discharge given by the velocity, v, in the inlet times the cross-sectional area, A, t is time, ∇P is a pressure gradient, C_d is the bottom friction coefficient, R_s is the radiation stress gradient in the cross-shore direction, b is the width of the inlet, ρ_a and ρ_w are the densities of air and water, respectively, and τ_w is the wind stress. The pressure gradient is given by

$$\nabla P = g \frac{\eta_o - \eta_B}{L} A \tag{2}$$

where g is the gravitational constant, η_o is the sea level in the sound or ocean and η_B is the sea level of the bay, and L is the inlet length. The bottom stress is estimated from a quadratic drag relationship, with the bottom friction coefficient estimated from observations (discussed below). The wave forcing in the ocean is given by the gradient in radiation stress, calculated as (Apotsos et al. 2008)

$$R_s = \frac{1}{16} g H_b^2 \frac{(\cos^2(\theta) + 0.5)}{\Delta x} \tag{3}$$

where H_b is the significant wave height (four times the standard deviation of sea-surface fluctuations between 0.05 and 0.30 Hz) at breaking, θ is the wave direction relative to the inlet channel axis, and Δx is the distance from the location of wave breaking to the inlet mouth. Wave radiation stress is assumed negligible in Vineyard Sound, and thus is neglected in the momentum equation for Edgartown Channel.

The wind stress, τ_w is calculated by (Large and Pond 1981)

$$\tau_w = C_{dw} |u_{10}| \, u_{10} \tag{4}$$

where C_{dw} is the drag coefficient for wind over water and u_{10} is the along-inlet component of the wind velocity at 10 m above the water–air interface. Winds are assumed uniform over the model domain.

For the case considered here where there are two inlets (Fig. 2), each with different tidal forcing and geometry, momentum equations must be solved for the flow in both inlets. Conservation of mass (continuity) implies

$$\frac{\partial \eta_B}{\partial t} = \frac{Q_1 + Q_2}{A_B} \tag{5}$$

where the subscripts 1 and 2 refer to the discharge from each of the two inlets and A_B is the surface area of the bay. Thus, the two momentum Eq. (1) are coupled to each other via the continuity Eq. (5).

Momentum balances and continuity are applied simultaneously at Katama Inlet and Edgartown Channel. The model is driven with sea level fluctuations owing to tides, storm surge, and other large scale processes observed in the ocean (MVCO, Fig. 1) and sound (sensor 01, Figs. 1 and 2), waves observed in 12 m depth offshore of Katama Inlet (MVCO, Fig. 1), and winds observed near the shore onshore of MVCO. Ten-minute averages of observed quantities were interpolated to 1-min values to drive the model, which was integrated in time using forward differences with 1-min time steps. Estimates for bottom friction and inlet dimensions come from field data, described in Section 3. Model output includes water levels in the bay and velocities through each inlet channel, which are averaged over 10 min to match the 10-min averages used for the observations.

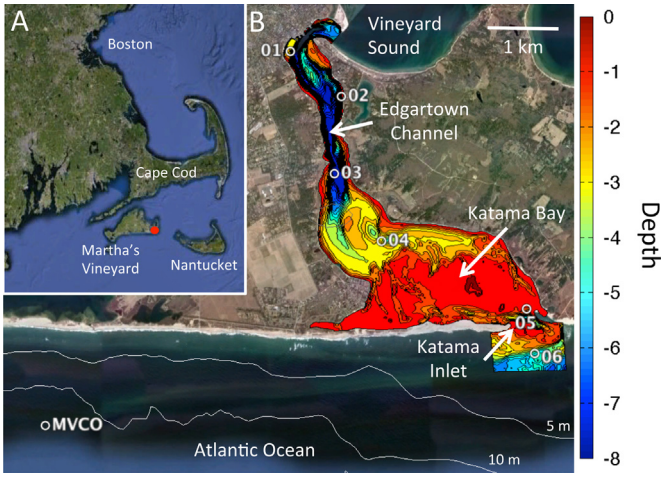

Fig. 1. Map of site location: (A) Google Earth image of eastern Massachusetts, Cape Cod, Nantucket, and Martha's Vineyard. The red circle indicates the location of Katama Bay. (B) Katama Bay, located on the eastern edge of Martha's Vineyard, and the surrounding nearshore region offshore of Katama Inlet. Water depth is indicated by the color contours (scale on the right) and contour curves (labeled with depth). Symbols indicate pressure sensors (01, 02), colocated pressure and current sensors (04, 05, 06), and colocated pressure sensors and current profilers (03, MVCO). The Martha's Vineyard Coastal Observatory (MVCO) observations were obtained in 12-m water depth.

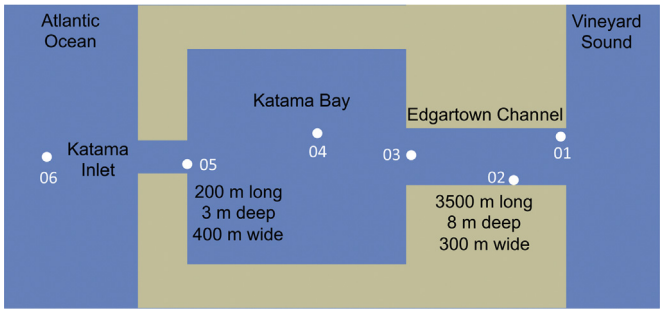

Fig. 2. Schematic of the model domain. The inlet and bay dimensions were obtained from bathymetric surveys with GPS and sonar on a wave runner and on a small boat. The model is driven with sea level observed in the sound (01) and in the ocean (MVCO, 12-m depth, Fig. 1), waves observed at MVCO, and winds observed near the shore onshore of MVCO. The model outputs are sea level in the bay (05) and velocities in Edgartown Channel (03) and Katama Inlet (05).

3. Observations and data collection

3.1. Location description

Katama Bay is located on Martha's Vineyard, an island south of Cape Cod (Fig. 1A). Martha's Vineyard and Nantucket Islands form a barrier between the open Atlantic Ocean to the south and east and Vineyard Sound to the north (Fig. 1A), resulting in spatially complex tidal patterns (Shearman and Lentz, 2004; Chen et al., 2011). The bay has a surface area of approximately 7.5×10^6 m^2,

Author's personal copy

and water depths range from 10 m at the north end where it connects to Edgartown Channel (sensor 03, Fig. 1) to less than 1 m in the southern half (red contours in Fig. 1). There is no major source of fresh water, and the waters are well mixed, with salinity about 32 PSU throughout the system.

3.2. Measurements

3.2.1. Surveys and inlet dimensions

The bay, inlet channels, and ebb shoal were surveyed with GPS and sonar mounted on a wave runner (Fig. 1). In addition, detailed cross-sections of the inlet channels were obtained with GPS and sonar mounted on a small boat (Fig. 3). The channel geometries were approximated with triangles that preserve the cross-sectional area (Fig. 3). The surveys and approximations provide the dimensions of the inlets (L, A, b) and bay (A_B) used in the model. Katama Inlet is 2 to 6 m deep, approximately 300 m long, and 400 m wide (Fig. 3B), whereas Edgartown Channel is 2 to 10 m deep, approximately 2500 m long, and 350 m wide (Fig. 3A). The widths and depths of the channels (and the triangular approximations, Fig. 3) depend on the sea level within the channel, which is estimated as the average depth between the bay and the ocean (Katama Inlet) or the sound (Edgartown Channel).

3.2.2. Hydrodynamic observations

Observations were obtained between mid August and early October 2011 at locations 01, 02, 03, 04, and 05, from mid September until early October at 06, and again for several days during the passage of Hurricane Sandy in late October 2012 at locations 01 and 05 (see Fig. 1 for locations). Pressure gages were mounted near the seafloor at all sensor locations, and were colocated with an acoustic Doppler current profiler (ADCP) in 10 m depth where Edgartown Channel meets the bay (03), and with acoustic Doppler velocimeters (ADV) in Katama Inlet (05) and on the outer edge of the ebb shoal in approximately 5 m depth (06). The pressure gages and ADVs were sampled at 2 Hz, and the ADCP samples were 1-min averages. Bottom pressures were corrected for atmospheric pressure fluctuations and converted to sea-surface elevation fluctuations assuming hydrostatic pressure and using linear theory. The ADV sample volumes were approximately 0.8 m above the sandy bottom. The flows at sensor 05, which is on the northern end of Katama Inlet, are assumed to represent the inlet currents, and the water levels at sensor 05 are used as a proxy for the bay water levels. In addition, water levels, significant wave heights, wave spectra, and wave directions were obtained in 12-m water depth (MVCO, Fig. 1), and wind was measured near the shoreline onshore of the 12-m depth sensors.

3.2.3. Waves

Incident (12-m water depth) significant wave heights ranged from 0.3 to 5.5 m (Fig. 4A), peak periods from 5 to 12 s, and mean wave directions from 160 to 210 degrees (close to normally incident on the south facing beaches surrounding the mouth of Katama Inlet). Waves in Vineyard Sound and especially in Edgartown Harbor were small, and are neglected here. Winds ranged from 0 to 17 m/s (Fig. 4B).

Waves measured in 12 m depth (MVCO, Fig. 1) were shoaled over the measured bathymetry (Fig. 1) to the depth at breaking assuming that linear energy flux EC_g is conserved, where E is the wave energy and C_g is the group velocity. Waves are estimated to begin to break when $\gamma = H_b/h = 0.8$, where h is the water depth. Different values of γ do not affect the results significantly. Comparison with waves measured in 5-m water depth on the ebb shoal (sensor 06 in Fig. 1) for the latter part of the 2011 observational period suggest shoaling the waves measured in 12-m depth to breaking is a reasonable approximation, and produces estimates of radiation stress gradients similar to those using the 5 m depth observations. Model results using the shoaled MVCO waves are not significantly different than those using the waves observed on the ebb shoal (06).

3.3. Bottom friction

The seafloor in Katama Inlet is sandy, with large (up to 1-m high and 10-m long) migrating bedforms reported by SCUBA divers, whereas the bottom in Edgartown Channel is smoother, and consists of harder, relatively immobile compacted finer sediments. Thus, the bottom friction coefficients of the two inlet channels may differ, and were estimated independently. Specifically, assuming a quadratic drag law, bottom friction coefficients, C_d, were estimated as the slope

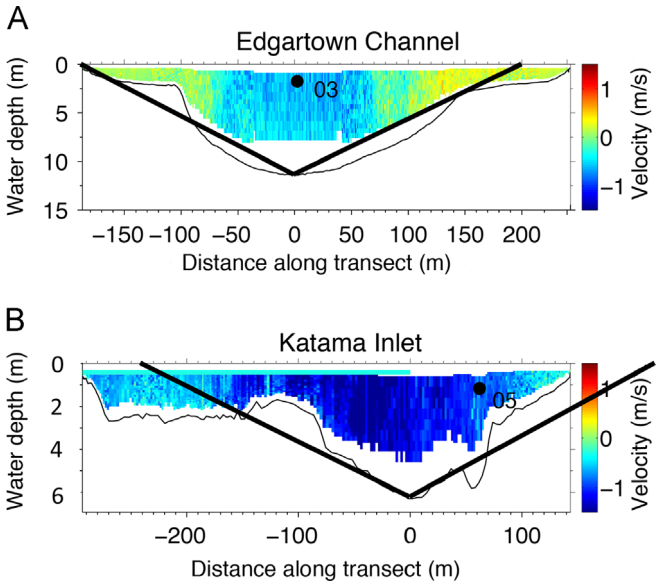

Fig. 3. Water depth (thin black curves) and velocity (color contours, scale on the right) across the (A) Edgartown and (B) Katama inlet channel axes versus along-transect distance from the center of the channel. Thick black triangles are the approximations to the bathymetry used to estimate channel cross-sectional areas in the model. Positive velocity is northward flow (into the page) and negative velocity is southward flow (out of page). The currents were measured with an acoustic Doppler profiler mounted on a small boat with GPS that traversed the channels slowly (approximately 1 m/s). Simultaneous depth soundings were obtained with a vertical sonar beam. The black circles are the horizontal locations of the sensors in Edgartown Channel (03) and Katama Inlet (05).

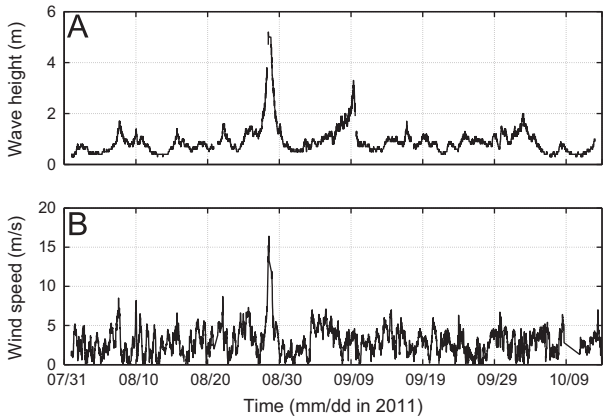

Fig. 4. Field conditions: (A) Significant wave height (0.05 to 0.30 Hz) and (B) wind speed versus time. Waves were measured in 12-m water depth (MVCO, Fig. 1), and winds were measured near the shoreline onshore of MVCO.

Author's personal copy

of a linear fit to pressure gradient versus $v|v|$ (Brown and Trask, 1980; Campbell et al., 1998; Giese and Jay, 1989; Kim et al., 2000), where the pressure gradients were between sensors 02 and 04 (Edgartown Channel, Fig. 1) and between sensors 04 and 06 (Katama Inlet, Fig. 1), with velocity v measured between the pressure sensors at locations 03 (Edgartown Channel) and 05 (Katama Inlet). The fits were obtained when waves were small. The drag coefficients were C_d=0.007 at Edgartown and C_d=0.011 at Katama. These estimates are similar to those obtained from the profiling current meter assuming a logarithmic boundary layer for the relatively few cases with a good fit (Kim et al., 2000), and to estimates based on the variance of the vertical velocities at sensor 05 (Nezu and Rodi, 1986; Elgar and Raubenheimer, 2010).

4. Model-data comparisons

Tidal sea-level fluctuations observed in the ocean are larger than, and several hours out of phase with those observed in the sound (Shearman and Lentz, 2004; Chen et al., 2011). Bay water levels observed near Katama Inlet (at 05) are between the ocean and sound water levels (Fig. 5A). For mild wave conditions, the model predicts accurately the observed bay water levels (Fig. 5B) whether or not wave forcing is included. During Hurricane Irene (Aug 28) incident significant wave heights were greater than 5 m, and the model predictions of bay water levels are more accurate when wave forcing is included (Fig. 5B). Unlike previous numerical results (Olabarrieta et al., 2011; Dodet et al., 2013), the increase in the bay water level owing to wave forcing is relatively small, as discussed below, likely because water flows out of the bay into Vineyard Sound through Edgartown Channel rather than accumulating in a closed basin.

In contrast to the bay water levels, wave forcing has a significant effect on the flows through Katama Inlet. Before (Aug 26–27) and after (Aug 29–30) the passage of Hurricane Irene (Aug 28) waves were moderate (Fig. 4), and both the model with and the model without waves predict the observed currents (Fig. 5C). However, during Hurricane Irene (Aug 28), wave forcing resulted in enhanced flood flows and reduced (almost to zero) ebb flows, which is predicted by the model with waves, but not by the model without waves (Fig. 5C). Simultaneously, during the hurricane the reduction in southward currents from the sound to the bay through Edgartown Channel is modeled more accurately if wave forcing is included than if waves are neglected (Fig. 5D). Ten days after the passage of Hurricane Irene, an offshore nor'easter storm produced waves greater than 3 m (September 9, Fig. 4A), resulting in enhanced flows into Katama Inlet that are predicted well by the model with wave forcing (not shown).

Although both Hurricane Irene and Hurricane Sandy had similar maximum wave heights (~5 m in 12-m water depth), the biggest waves of Hurricane Irene occurred during low tide in the ocean (ebb flows in Katama Inlet, negative current speed, mid-day of Aug 28, Fig. 5C) and the biggest waves of Hurricane Sandy occurred during high tide in the ocean (late-day of Oct 29, Fig. 6C). Similar to Irene, model simulations suggest that waves force ocean water into the bay during Sandy (Fig. 6C, compare red with blue curves). Strong easterly winds during Sandy produced elevated water levels at tide stations throughout Vineyard Sound (not shown), with some of the highest levels observed in Edgartown Channel, resulting in an extended period of high water levels during the storm (Fig. 6A), and a corresponding decrease in the flood flow at Katama Inlet (Fig. 6C). Without considering the effect of waves, the model predicts an ebb flow at Katama Inlet during the peak of Hurricane Sandy instead of the observed flood flow (Fig. 6C, late on Oct 29). The model with waves predicts the weak flood flows, similar to the observations at the inlet. This change in sign could have significant impacts on sediment transport and discharge.

During the observational period there were several events with significant wave heights greater than about 2 m (Fig. 4A and Hurricane Sandy). As wave heights increase, the root mean square errors between observed currents in Katama Inlet and those predicted by the model without waves increase, whereas the root mean square errors in currents simulated by the model with wave forcing remain approximately constant (Fig. 7). For energetic waves the errors in the model with wave forcing are about one-half as large as those for the model without wave forcing.

The model simulations and the observations are consistent with the hypothesis (Bertin et al., 2009; Malhadas et al., 2009; Olabarrieta et al., 2011; Dodet et al., 2013) that wave forcing is important to circulation near an inlet. However, unlike previous

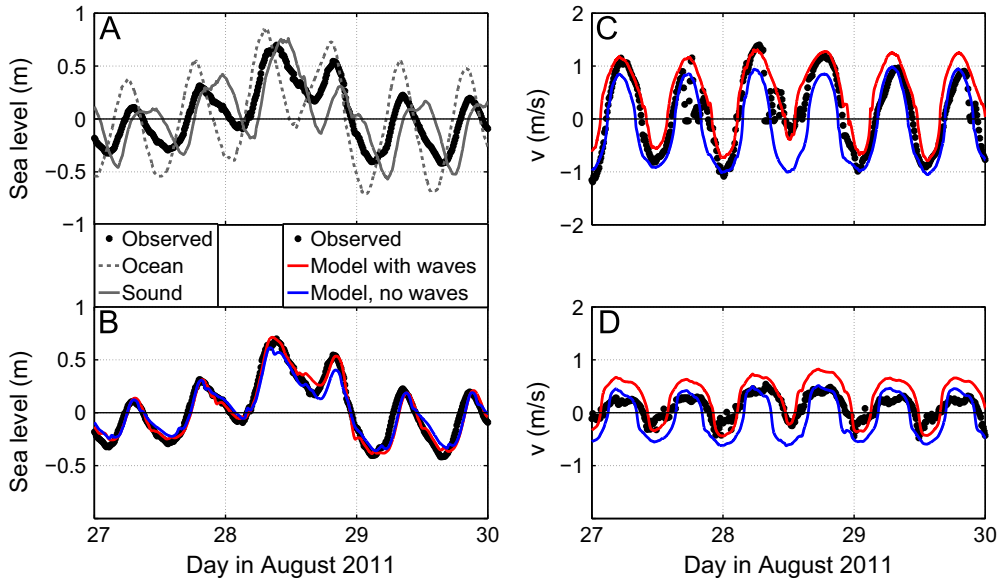

Fig. 5. Model-data comparison for Hurricane Irene: (A) Sea level observed in the Atlantic Ocean (dashed grey curve), Vineyard Sound (solid grey curve), and in the bay near Katama Inlet (black dots, sensor 05 in Fig. 1), and observed (black) and modeled (blue is model without waves, red is model with waves) (B) bay sea level near Katama Inlet (05), (C) velocity in Katama Inlet (05), and (D) velocity in Edgartown Channel (03) versus time. Positive velocity is northward flow (i.e., from the ocean to the bay and from the bay to the sound). Hurricane Irene was Aug 28, 2011.

Author's personal copy

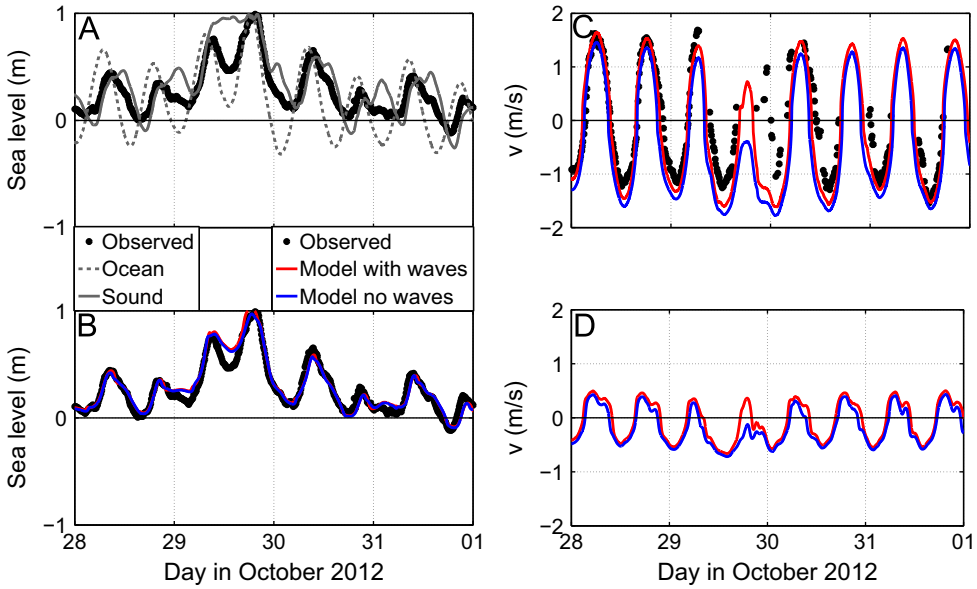

Fig. 6. Model-data comparison for Hurricane Sandy: (A) Sea level observed in the Atlantic Ocean (dashed grey curve), Vineyard Sound (solid grey curve), and in the bay near Katama Inlet (black dots, sensor 05 in Fig. 1), and observed (black) and modeled (blue is model without waves, red is model with waves) (B) bay sea level near Katama Inlet (05), (C) velocity in Katama Inlet (05), and (D) velocity in Edgartown Channel (03) versus time. Positive velocity is northward flow (i.e., from the ocean to the bay and from the bay to the sound). Hurricane Sandy was Oct 29, 2012.

numerical studies of inlets connecting enclosed basins with the ocean, in this two-inlet system wave radiation stresses resulted in only a small increase in bay water levels (Figs. 5 and 6). For a closed basin, the water forced into the inlet by wave radiation stresses produces increased bay water levels and a seaward pressure gradient. For Katama, the increased flow from the ocean into the bay can continue to flow northward through Edgartown Channel into Vineyard Sound (Fig. 1). The observed net discharge from Aug 25 until Sep 25, 2011 was from the ocean through the bay to the sound, opposite to the net discharge predicted by the numerical model without wave forcing. In contrast, the net discharge predicted by the model with wave forcing was in the same direction as the observations, both during Hurricane Irene and over a 1-month period with a range of conditions (not shown).

5. Model errors

The wind stress term was significantly smaller than the other terms in the momentum balance (1), even during hurricanes, either owing to the local wind speed or to the wind direction. Similarly, the temporal changes in discharge also were much smaller than the other terms in the momentum balance (1). Thus, the dominant terms in the momentum balance are the pressure gradients between the sound, ocean, and bay, wave radiation stresses acting on Katama Inlet, and bottom stress owing to friction of the flows in the inlet channels.

The numerical model assumes inlet flows are uniform both in the vertical and across the inlet channel. Transects across the channels with an acoustic Doppler profiling current meter are consistent with the assumption of little vertical shear (Fig. 3), but indicate there is some horizontal shear, especially between the center of Edgartown Channel and the shoals on its sides (Fig. 3A). However, although possibly important to the three-dimensional circulation and to the discharge magnitude, the shear in Edgartown Channel does not affect the conclusion presented here based on the one-dimensional model that waves are important to the circulation.

The model depends on the geometry of the inlets and the bay. The bay surface area was obtained from wave runner-based bathymetric surveys (Fig. 1), which may not estimate the location of the shoreline accurately. Moreover, the cross-sections of the inlet channels are approximated as triangles (Fig. 3). However, numerical experiments (not shown) suggest the results are not sensitive to different approximations to the channel cross-section, including the triangular approximation used here.

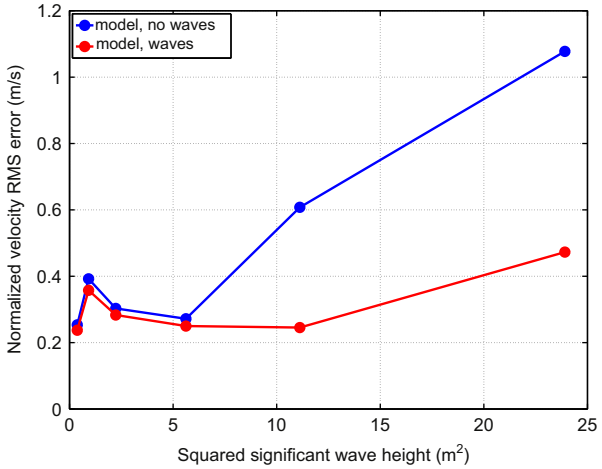

Fig. 7. Root mean square (RMS) error between modeled and observed velocity normalized by the root mean square of the observed velocity in Katama Inlet versus squared offshore significant wave height (proportional to radiation stress) for the model with (red curve) and without (blue curve) wave forcing.

During Hurricanes Irene and Sandy and the nor'easter storms, waves may have been breaking offshore of the MVCO site (Fig. 1), resulting in an underestimation of the radiation stress forcing, and thus an underestimation of the effects of wave forcing (e.g., the red curves in Fig. 5 during Hurricane Irene, Aug 28 and in Fig. 6 during Hurricane Sandy, Oct 29).

Although the one-dimensional model used here is sufficient to address the hypothesis (Bertin et al., 2009; Malhadas et al., 2009; Olabarrieta et al., 2011; Dodet et al., 2013) that wave forcing is important to inlet currents (Figs. 5 and 6), a more sophisticated model (Wheless and Valle-Levinson, 1996; Hench and Luettich, 2003; Olabarrieta et al., 2011) might produce more detailed results. For

Author's personal copy

example, the model used here assumes that the water level in the bay responds uniformly to the forcing at the two inlets, and that the measurements at location 05 represent the bay water levels. However, there were variations in the water levels observed along the bay between Katama Inlet and Edgartown Channel. Similarly, for the frictionally dominated shallow inlets and bay considered here, nonlinear advective acceleration terms are assumed to be small, or to cancel (Jay, 1991; Lentz et al., 1999; Olabarrieta et al., 2011), but are included in other models. Although beyond the scope of this study, a more sophisticated modeling approach could resolve possible tilts in the bay water level, as well as two- and three-dimensional flow structures in the system.

6. Conclusions

Observations of water levels, winds, waves, and currents in Katama Bay and Inlet are consistent with the hypothesis (Bertin et al., 2009; Malhadas et al., 2009; Olabarrieta et al., 2011; Dodet et al., 2013) that wave forcing is important to circulation in inlet channels and to water levels in the bay. A numerical model based on a balance of temporal changes in discharge, tidal- and surge-induced pressure gradients, and wave-radiation, wind, and bottom stresses, along with conservation of mass, predicts the currents observed in Katama Inlet more accurately when wave forcing is included than when waves are ignored. Including wave forcing reduces errors in model predictions of inlet current speeds to one-half the errors when waves are ignored.

During Hurricanes Irene and Sandy, wave radiation stresses caused enhanced flows into the bay during flood tides, and reduced (almost to zero during Irene) flows out of the bay during ebb tides. Unlike in closed basins, both the observed and modeled water levels in the bay did not increase greatly during storms, likely because water could flow from Katama Inlet through Edgartown Channel to Vineyard Sound. Consistent with observations, net discharge was from the ocean through the bay and out to the sound when waves are included in the model, but was in the opposite direction when waves were neglected. This wave-induced circulation pattern can lead to enhanced transport of sediments, nutrients, larvae, and other material into bays during storms, affecting navigation, water quality, shellfish farms, and possibly leading to closure of the inlet.

Acknowledgements

We thank Maria Brown, David Clark, Danik Forsman, Levi Gorrell, Jeff Hansen, Sean Kilgallin, Christen Rivera-Erick, Jenna Walker, Anna Wargula, Regina Yopak, and Seth Zippel for helping to obtain the data, Maddie Smith for drag coefficients based on vertical velocities, Janet Fredericks for help with the MVCO data, Clare Gesualdo, Charlie Blair, and the Edgartown Reading Room for providing pier pilings for pressure gages and moorings for small boats, and Mike Creato for providing staging space and a pleasant place to work at Katama Airpark. The Office of the Assistant Secretary of Defense for Research and Engineering, the National Science Foundation, and the Office of Naval Research provided funding.

References

Apotsos, A., Raubenheimer, B., Elgar, S., Guza, R., 2008. Wave-driven setup and alongshore flows observed onshore of a submarine canyon. J. Geophys. Res 113, C07025, http://dx.doi.org/10.1029/2007JC004514.

Aubrey, D., Giese, G. (Eds.), 1993. Formation and evolution of multiple tidal inlets. In: Coastal and Estuarine Studies, 44. AGU, Washington, DC, p. 238, http://dx.doi.org/10.1029/CE044.

Bertin, X., Fortunato, A., Oliveira, A., 2009. A modeling-based analysis of processes driving wave-dominated inlets. Cont. Shelf Res. 29, 819–834.

Brown, W., Trask, R., 1980. A study of tidal energy dissipation and bottom stress in an estuary. J. Phys. Oceanogr 10, 1742–1754.

Bruun, P., 1978. Stability of Tidal Inlets: Theory and Engineering. Elsevier.

Bruun, P., Adams, J., 1988. Stability of tidal inlets: use of hydraulic pressure for channel and bypassing stability. J. Coastal Res 4, 687–701.

Campbell, A., Simpson, J., Allen, G., 1998. The dynamical balance of flow in the Menai Strait. Estuarine Coastal Shelf Sci. 46, 449–455.

Chen, C., Huang, H., Beardsley, R., Xu, Q., Limeburner, R., Cowles, G., Sun, Y., Qi, J., Lin, H., 2011. Tidal dynamics in the Gulf of Maine and New England Shelf: an application of FVCOM. J. Geophys. Res 116, C12010, http://dx.doi.org/10.1029/2011JC007054.

Dodet, G., Bertin, X., Bruneau, N., Fortunato, A., Nahon, A., Roland, A., 2013. Wave-current interactions in a wave-dominated tidal inlet. J. Geophys. Res 118, 1587–1605.

Easton, M., Woolf, D., Bowyer, P., 2012. The dynamics of an energetic tidal channel, the Pentland Firth, Scotland. Cont. Shelf Res. 48, 50–60.

Elgar, S., Raubenheimer, B., 2010. Currents in a small channel on a sandy tidal flat. Cont. Shelf Res. 31, 9–14, http://dx.doi.org/10.1016/j.csr.2010.10.007.

Giese, B., Jay, D., 1989. Modeling estuary energetics of the Columbia River estuary. Estuarine Coastal Shelf Sci 29, 549–571.

Hench, J., Luettich, R., 2003. Transient tidal circulation and momentum balances at a shallow inlet. J. Phys. Oceanogr 33, 913–932.

Jay, D., 1991. Green's law revisited: tidal long-wave propagation in channels with strong topography. J. Geophys. Res 96, 20,585–20,598, http://dx.doi.org/10.1029/91JC01633.

Kim, S., Friedrichs, C., Maa, J., Wright, L., 2000. Estimating bottom stress in tidal boundary layer from acoustic Doppler velocimeter data. J. Hydraul. Eng. 126, 499–506.

LeConte, L., 1905. Discussion on the Paper, "Notes on the Improvement of River and Harbor Outlets in the United States" by D.A. Watt., Paper no. 1009, Transactions of ASCE 55 (December), pp. 306–308.

Large, W., Pond, S., 1981. Open ocean momentum flux measurements in moderate to strong winds. J. Phys. Oceanogr 11, 324–336.

Lentz, S., Guza, R., Elgar, S., Feddersen, F., Herbers, T., 1999. Momentum balances on the North Carolina inner shelf. J. Geophys. Res 104, 18,205–18,226.

Longuet-Higgins, M., 1970. Longshore currents generated by obliquely incident sea waves. J. Geophys. Res 75, 6778–6789.

Longuet-Higgins, M., Stewart, R., 1964. Radiation stresses in water waves: a physical discussion with applications. Deep Sea Res 11, 529–562.

Malhadas, M., Leitao, P., Silva, A., Neves, R., 2009. Effect of coastal waves on sea level in Obidos Lagoon, Portugal. Cont. Shelf Res. 29, 1240–1250.

Nezu, I., Rodi, W., 1986. Open-channel flow measurements with a laser Doppler anemometer. J. Hydraul. Eng. 112 (5), 335–355.

O'Brien, M.P., 1931. Estuary tidal prism related to entrance areas. Civil Eng. 1 (8), 738–739.

O'Brien, M.P., 1969. Equilibrium flow areas of inlets on sandy coasts. J. Waterw. Harbors Coast Eng. Div. ASCE 95 (1), 43–52.

Olabarrieta, M., Warner, J., Kumar, N., 2011. Wave–current interaction in Willipa Bay. J. Geophys. Res 116, C12014, http://dx.doi.org/10.1029/2011JC007387.

Proudman, J., 1953. Dynamical Oceanography. Methuen, London.

Salles, P., Voulgaris, G., Aubrey, D., 2005. Contribution of nonlinear mechanisms in the persistence of multiple tidal inlet systems. Estuarine Coastal Shelf Sci 65, 475–491.

Shearman, K., Lentz, S., 2004. Observations of tidal variability on the New England shelf. J. Geophys. Res 109, C06010, http://dx.doi.org/10.1029/2003JC001972.

Stevenson, T., 1886. Design and Construction of Harbours, third ed.. Adam and Charles Black, Edinburgh.

Stevens, C., Sutton, P., Smith, M., Dickson, R., 2008. Tidal flows in Te Aumiti (French Pass), South Island, New Zealand. N.Z. J. Mar. Freshwater Res. 42, 451–464.

van de Kreeke, J., Brouwer, R., Zitman, T., Schuttelaars, H., 2008. The effect of a topographic high on the morphological stability of a two-inlet bay system. Coastal Eng. 55, 319–332.

Wheless, G., Valle-Levinson, A., 1996. A modeling study of tidally driven estuarine exchange through a narrow inlet onto a sloping shelf. J. Geophys. Res. 101, 25,675–25, 687.